Atmospheric Environment 234 (2020) 117583

Contents lists available at ScienceDirect

Atmospheric Environment

journal homepage: http://www.elsevier.com/locate/atmosenv

Tibetan Plateau driven impact of Taklimakan dust on northern rainfall

Yuzhi Liu [a,b,*], Qingzhe Zhu [b], Shan Hua [b], Khan Alam [c], Tie Dai [d], Yueming Cheng [d]

[a] Collaborative Innovation Center for Western Ecological Safety, Lanzhou University, Lanzhou, 730000, China
[b] College of Atmospheric Sciences, Lanzhou University, Lanzhou, 730000, China
[c] Department of Physics, University of Peshawar, Peshawar, 25120, KPK, Pakistan
[d] LASG, Institute of Atmospheric Physics, Chinese Academy of Sciences, Beijing, 100029, China

HIGHLIGHTS

- Effects of Taklimakan dust on the cloud and rainfall surrounding the TP are simulated.
- Taklimakan dust can decrease the CER but increase the COD, LWP and IWP over the TP.
- Eastward movement of the dust-polluted clouds over the TP can intensify the rainfall over the northern area.

ARTICLE INFO

Keywords:
NICAM
Tibetan plateau
Taklimakan desert
Dust
Clouds
Rainfall

ABSTRACT

In our previous study (Li et al., 2019a), using observational data, we found some evidences of Taklimakan dust effects on the convective clouds over the Tibetan Plateau (TP) and then causing heavy rainfall in the downstream region. Here, a simulation study is performed to quantify the effects of Taklimakan dust on the cloud properties over the TP and downstream rainfall using the Spectral Radiation-Transport Model for Aerosol Species (SPRINTARS) coupled to the Nonhydrostatic Icosahedral Atmospheric Model (NICAM). The results indicate that the dusts in Taklimakan desert can be lifted to the northern slope of the TP. The dust aerosols transported to the TP can diminish the cloud effective radius (CER), but they can increase the cloud optical depth (COD), liquid water path (LWP) and ice water path (IWP) over the TP. The maximum impact of the dusts on the CER lags behind the peak of aerosol optical depth (AOD). Meanwhile, the dusts show a more profound impact on the ice-cloud optical depth (ICOD) than liquid-cloud optical depth (LCOD), which implies a more significant impact on the ice particles than liquid drops in convective clouds over the TP. Overall, due to the indirect effects of Taklimakan dust aerosols, the clouds are developed further over the TP. The eastward movement of the clouds polluted by Taklimakan dust can delay the occurrence of heavy rainfall for 12 h but intensify the rainfall over the northern area. This modeling study verified and quantified the indirect effect of Taklimakan dusts on the cloud properties over the TP and further impacts on the rainfall over the northern area.

1. Introduction

Atmospheric aerosols are intrinsically linked to climate change, air quality and human health (Segal et al., 1989; Feingold et al., 2005; Garrett and Zhao, 2006; Zhang, 2010; Xie et al., 2013; Liu et al., 2014; Zhao and Garrett, 2015; Zhu et al., 2018; Li et al., 2019; Zhao et al., 2020). Aerosols can change the energy balance of the earth-atmosphere system by interacting with solar radiation (Sokolik and Toon, 1996; Lau et al., 2006; Liu et al., 2011, 2013; Huang et al., 2014; Yang et al., 2016a, 2018a), which can change the thermal structure of atmosphere and further affect cloud properties and precipitation (Ramanathan et al., 2005; Meehl et al., 2008; Benedetti et al., 2009; Jin et al., 2014; Yang et al., 2016b, 2018b; Zhao et al., 2018). Some aerosols produced by fossil fuel combustion and biomass burning, such as black carbon and organic carbon, can change relative humidity and evaporate clouds, and thus affect precipitation due to their absorption properties (Huang et al., 2006a, 2010; Fan et al., 2008; Sakaeda et al., 2011; Jiang et al., 2018; Lu et al., 2018). Meanwhile, aerosols can also affect the cloud microphysical properties and precipitation by interacting with clouds (Twomey, 1977; Albrecht, 1989; Ackerman et al., 2000; Feingold et al., 2005; Huang et al., 2006b; van den Heever et al., 2006; Morrison and Grabowski, 2011; Guo et al., 2014; Liu et al., 2019a, 2019b). Indeed,

* Corresponding author. Collaborative Innovation Center for Western Ecological Safety, Lanzhou University, Lanzhou, 730000, China.
E-mail address: liuyzh@lzu.edu.cn (Y. Liu).

https://doi.org/10.1016/j.atmosenv.2020.117583
Received 9 February 2020; Received in revised form 20 April 2020; Accepted 1 May 2020
Available online 8 May 2020

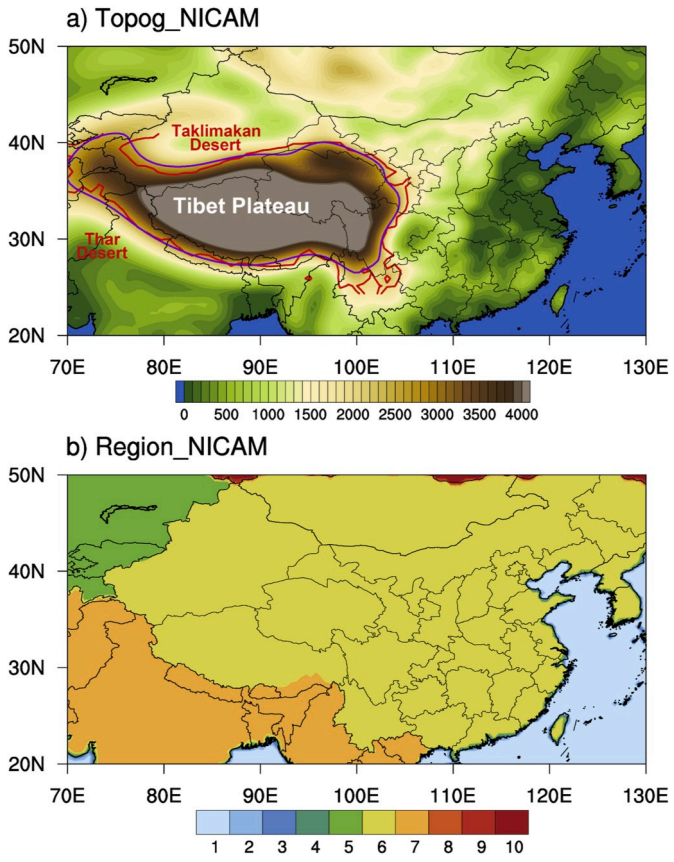

Fig. 1. (a) Spatial topographical in meter (above mean sea level) and (b) NICAM defined regions. The purple and red lines in panel (a) indicate the main areas of the TP in NICAM and geophysical data, respectively. (For interpretation of the references to colour in this figure legend, the reader is referred to the Web version of this article.)

Table 1
Coefficients of dust emission and critical values of soil moisture for the regions in this study.

Region	Coefficients of dust emission	Soil moisture
1	0.0	0.1
5	2.0×10^{-9}	0.1
6	1.85×10^{-9}	0.2
7	4.0×10^{-9}	0.15
10	0.0	0.1

aerosol-radiation-cloud interaction is an important issue in the research of atmospheric physical process and climate change.

On the impact of aerosols on the rainfall, much effort has been made. Basing on observations and model simulations, Guo et al. (2016) and Lee et al. (2016) reported that the reduction of solar radiation at the surface under heavy pollution conditions can delay the occurrence of strong convection and postpone heavy precipitation over southern China. Fan et al. (2015) found that aerosols can increase atmospheric stability and inhibit convection by absorbing solar radiation during daytime, which could generate strong convection and trigger extremely heavy precipitation at night because of the moisture transport to mountain area. On the other hand, it was found that the aerosol-cloud interaction can change the rainfall location, intensity, and type (Tao et al., 2012; Zhao et al., 2018). Rosenfeld et al. (2011) found that the dust aerosols and air pollution in East Asia have impacts on ice precipitation. Fan et al. (2014) found that dust and biological aerosols over California can enhance the accumulated precipitation by 10–20%. Besides, many other studies have pointed out that due to the effects of aerosols, the drizzle and light rain is suppressed (Rosenfeld et al., 2001; Andreae et al., 2004; Khain et al., 2008; Li et al., 2016) and heavy rain is enhanced (Zhang and Gao, 2007; Min et al., 2009; Li et al., 2011; Koren et al., 2012).

The Tibetan Plateau (TP), acting as an important role in adjusting the weather and climate at regional and global scales (Liu et al., 2020), is surrounded by several important natural and anthropogenic aerosol sources (Jia et al., 2015; Zhao et al., 2020). Driven by meteorological circulations, the aerosols can be transported over long-distance. So, they can affect the weather and climate not only in source area but in transport areas (Rajeev et al., 2000; Huang et al., 2014; Liu et al., 2019c, 2019d; Zhu et al., 2020). Previous studies have found that aerosols can be transported to the TP (Huang et al., 2007; Jia et al., 2018, 2019; Fan et al., 2020; Pokharel et al., 2020), where dust is the major type of aerosols over the northern TP (Zhang et al., 2001). Moreover, satellite observations and model simulations have shown that dust aerosols over northern slope of the TP mainly originate from the Taklimakan desert (Huang et al., 2007; Jia et al., 2015; Liu et al., 2015). These dust aerosols would affect the radiation budget (Huang et al., 2009; Kuhlmann and Quaas, 2010; Lau et al., 2010) and further affect meteorological fields over the TP (Yang et al., 2017; Yuan et al., 2019). Recent studies indicate that due to the special topography of the TP, the effect of aerosols on clouds over the TP is stronger than that over northern China (Zhou et al., 2017), and the eastward movement of polluted-clouds by dusts over the TP can further alter the rainfall in the downstream region (Liu et al., 2019a). However, there exist some uncertainties in separating out the impacts of Taklimakan dusts on the cloud properties over the TP and subsequent impacts on the downstream rainfall.

To quantify the impact of Taklimakan dusts, we perform two groups of experiments for a dusty event accompanied rainfall in the vicinity of the TP using the Nonhydrostatic Icosahedral Atmospheric Model (NICAM) coupled with the Spectral Radiation-Transport Model for Aerosol Species (SPRINTARS). The Moderate Resolution Imaging Spectroradiometer (MODIS) data, China Meteorological Administration (CMA) data and Copernicus Atmosphere Monitoring Service (CAMS) reanalysis data are used to evaluate the simulative ability of model. This paper is organized as follows, the data and model used in this study are described in Section 2 and Section 3, respectively; the simulations from NICAM are evaluated by comparing with the observations and reanalysis data in Section 4, and the impacts of aerosols on the cloud properties and downstream precipitation are analyzed in Section 5; In Section 6, the conclusions are summarized and discussed.

2. Observational and reanalysis data

2.1. Moderate resolution imaging spectroradiometer (MODIS) products

MODIS instruments aboard the two earth observing system satellites Terra and Aqua provide global aerosol and cloud observations (Platnick et al., 2003; Remer et al., 2005). In this study, the dark target and deep blue combined aerosol optical depth retrievals from the MOD04_L2 and MYD04_L2 products with a spatial resolution of 10 × 10 km are used to evaluate the aerosol distribution simulated by the model over study area, both kinds of products are combined to fill the spatial gaps left by one another during satellite passes. Cloud parameters including cloud fraction (CF) and cloud optical depth (COD) derived from MOD08_D3 product with a horizontal resolution of 1° × 1° during 15–19 July 2016 are used to evaluate the simulated cloud property over the study area.

2.2. China meteorological administration (CMA) products

The China Meteorological Data Service Center (http://data.cma.cn/en) which provides meteorological data across China and the world is an authoritative and unified shared service platform of CMA (Ying et al., 2014). In this study, hourly precipitation, integrated by China automatic stations and the climate prediction center morphing method (Joyce et al., 2004) with a resolution of 0.1° × 0.1° during

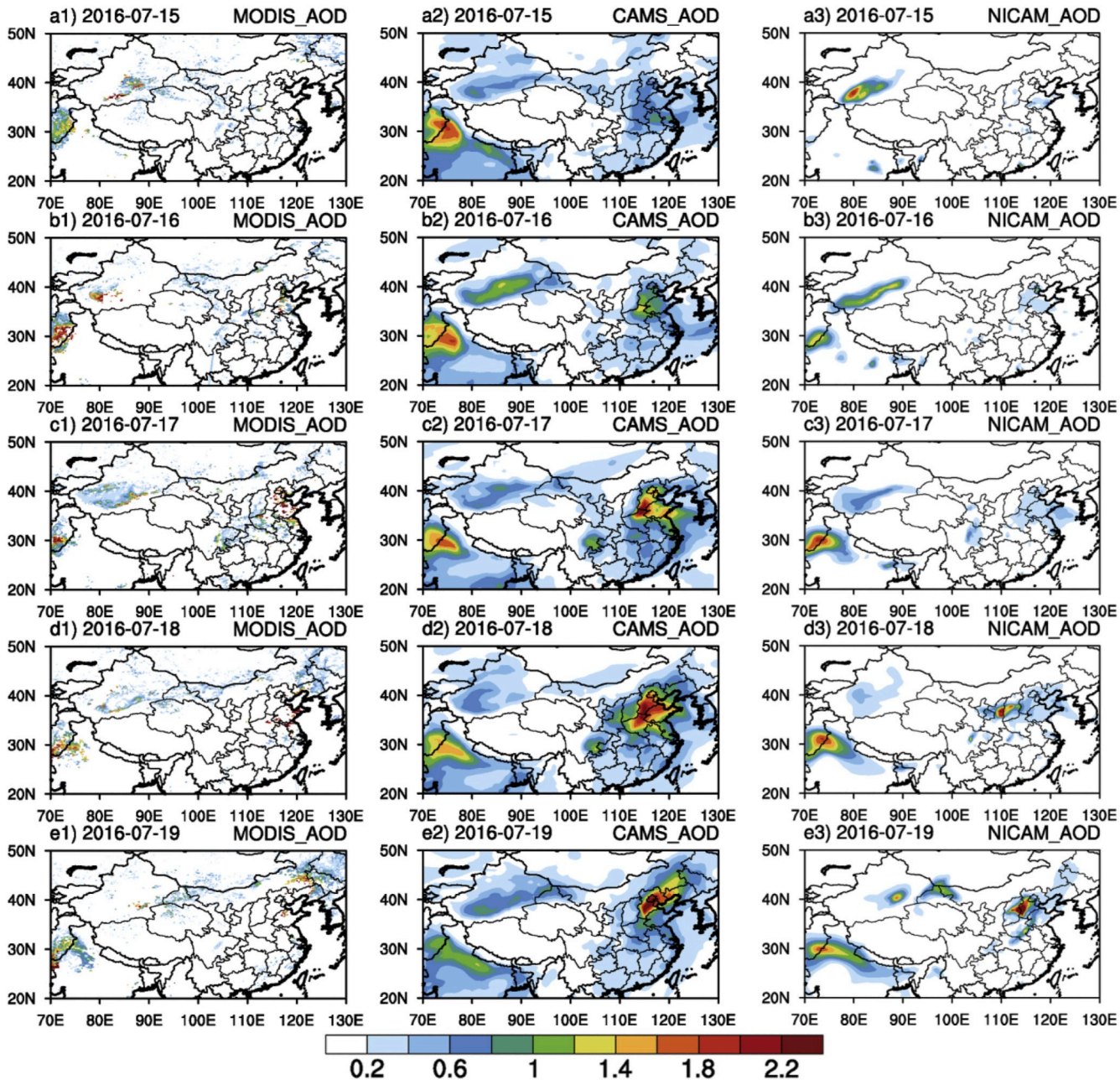

Fig. 2. Distributions of daily mean AOD derived from (a1-e1) MODIS observation, (a2-e2) CAMS reanalysis data and (a3-e3) NICAM simulation during 15–19 July 2016.

15–19 July 2016 is used to compare with the simulated precipitation by model.

2.3. Copernicus Atmosphere Monitoring Service (CAMS) products

CAMS, which is operated by the European Centre for Medium-Range Weather Forecast (ECMWF), provides reliable products regarding the composition and variations of the atmosphere. Among these products, the reanalysis product of AOD at 550 nm is provided by the forward model C-IFS, assimilating data from the MODIS instruments on the Aqua and Terra satellites (Benedetti et al., 2009). In this study, the data of AOD at 550 nm with a spatial resolution of 0.5° × 0.5° during 15–19 July 2016 are used to compare the simulated AOD by model.

3. Model description

3.1. NICAM and SPRINTARS

The NICAM (Tomita and Satoh, 2004; Satoh et al., 2008, 2014) coupled online with the SPRINTARS (Suzuki et al., 2008) is used in this study. Using a non-hydrostatic dynamic core and an icosahedral grid configuration, NICAM can be adapted to run with flexible horizontal resolutions of low (approximately 200 km) to high (approximately 1 km) (Miyamoto et al., 2013; Dai et al., 2014a). Higher resolution grids are stretched from a coarser resolution grid (Dai et al., 2014b; Goto et al., 2017), which can enable NICAM to simulate at high resolutions in specific areas (Goto et al., 2015a).

The aerosol module called SPRINTARS reconciled with NICAM is a global 3-D aerosol radiation transport model (Takemura et al., 2000, 2002, 2009). In order to study the effects of aerosols on radiation and

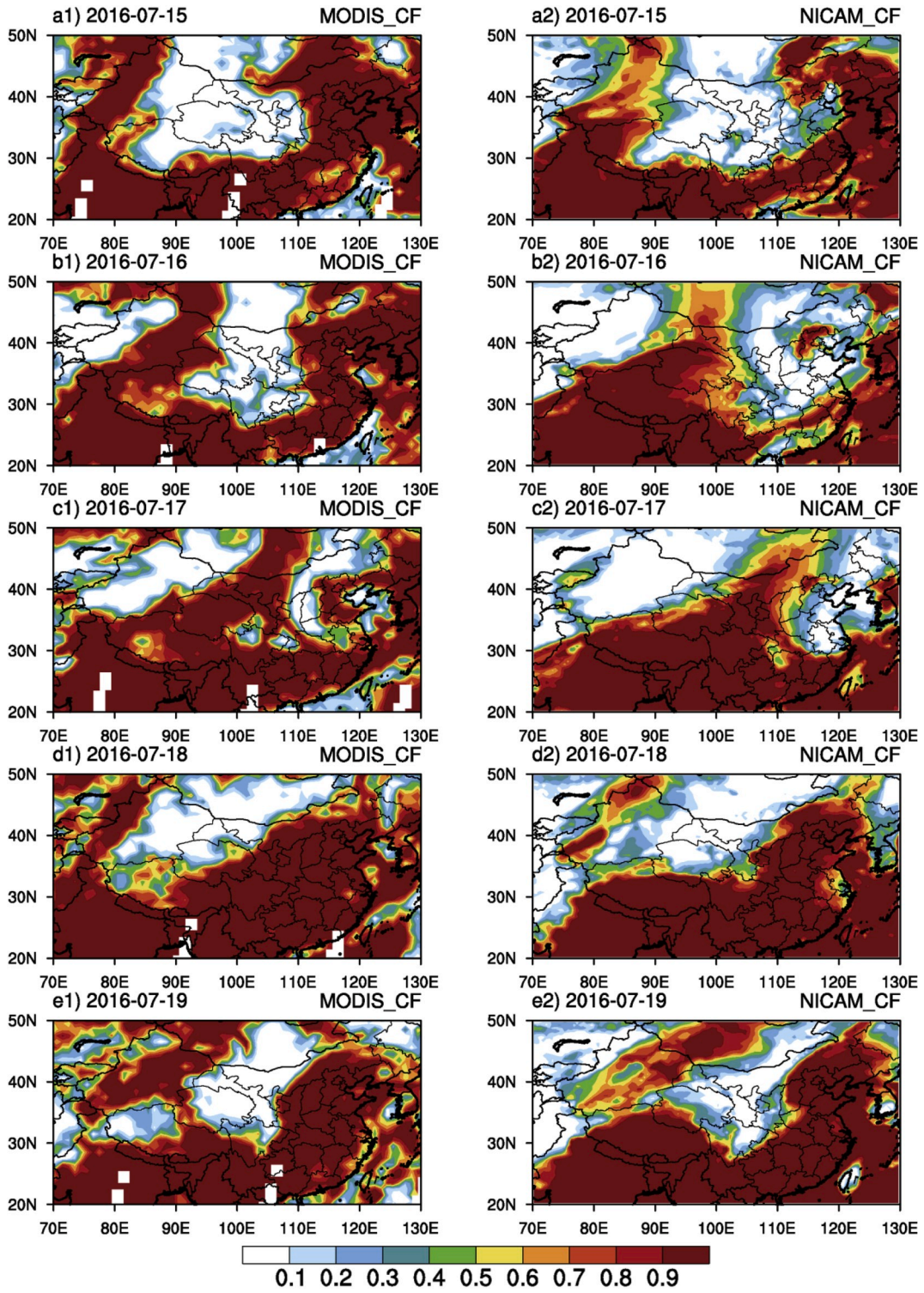

Fig. 3. Distributions of daily mean cloud fraction derived from (a1-e1) MODIS observation and (a2-e2) NICAM simulation during 15–19 July 2016.

cloud properties, the direct and indirect effects of aerosols are taken into account in this aerosol-coupled version of NICAM (Suzuki et al., 2008, 2011). In NICAM-SPRINTARS, aerosol mass of sulfate and carbonaceous aerosols (black carbon and organic carbon) are predicted by considering the emission, transport, and deposition processes (Dai et al., 2015; Takemura et al., 2000). The emission inventories used in this model are from the AeroCom-II ACCMIP datasets (Lamarque et al., 2010). Sea salt is tracked in 4 bins and the emissions are calculated online mainly depending on the near-surface wind speeds (Takemura et al., 2009). The dust aerosols are divided into 10 bins ranging from 0.1 to 10 μm (Takemura et al., 2000). The emission of dust is calculated according to the following conditions: (1) wind speeds at the 10-m height are greater than 2.5 m/s, (2) soil relative moisture is less than threshold moisture for specific regions, (3) emission factors for specific regions and (4) surface snow amount is less than 1 kg/m^2.

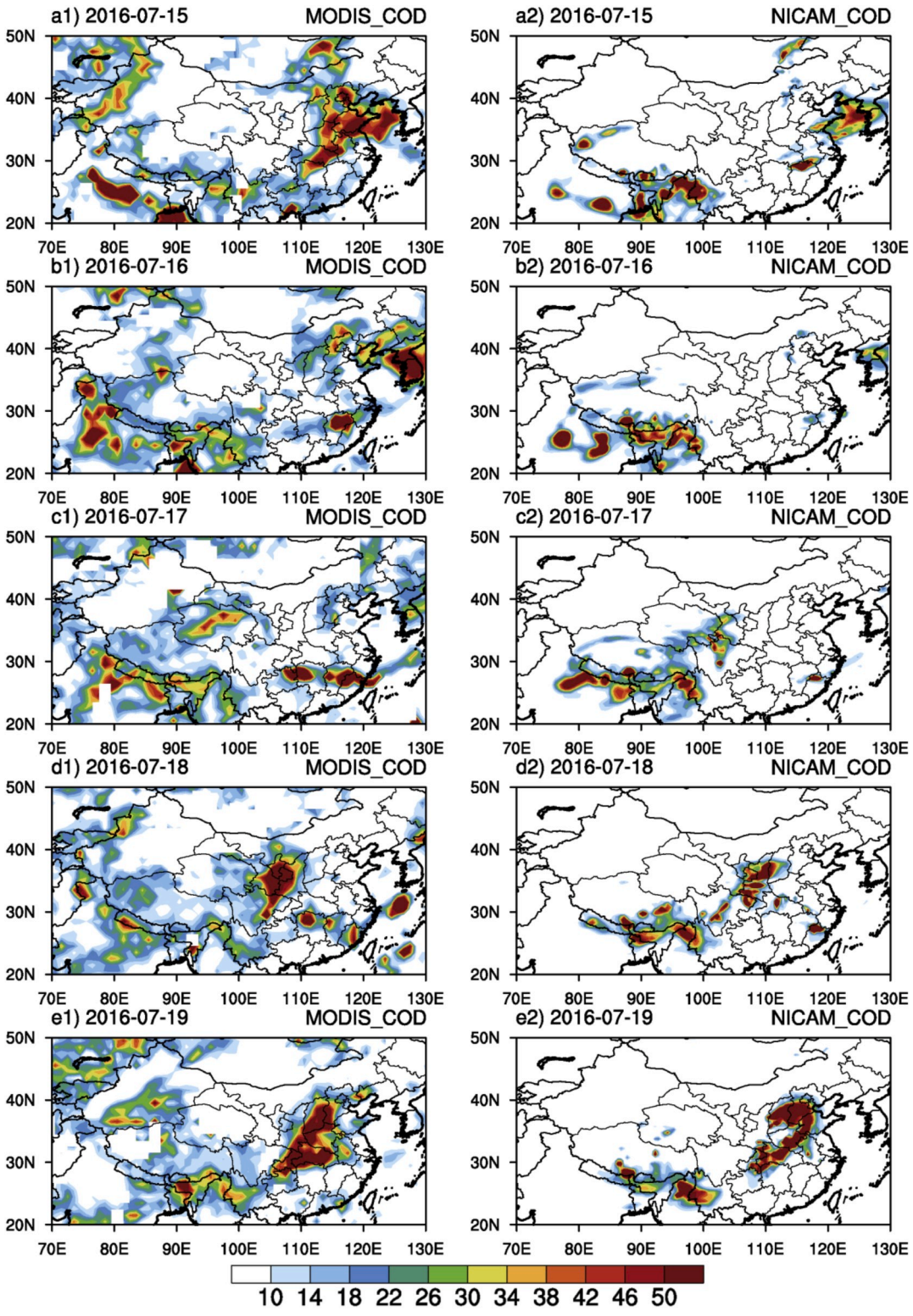

Fig. 4. Same as Fig. 3, but for cloud optical depth.

3.2. Experimental set up

In this study, global coarse grids are set as 56 km, center position is set at 35°N, 110°E and the stretching factor is 64, which results in a resolution of about 7 km in the study area (Fig. 1a). Vertically, a total of 40 levels are established from the surface to approximately 40 km altitude.

The model divides the world into 10 regions to set the emission coefficient and critical values of soil moisture respectively (Dai et al., 2018), the indices of the dust emission regions used in this study are 1, 5, 6, 7 and 10 (Fig. 1b). The corresponding emission factors and soil moisture are listed in Table 1. The cloud microphysics module used in this study is a single-moment type with six categories (NSW6) including water vapor, cloud water, rain, cloud ice, snow, and graupel (Tomita,

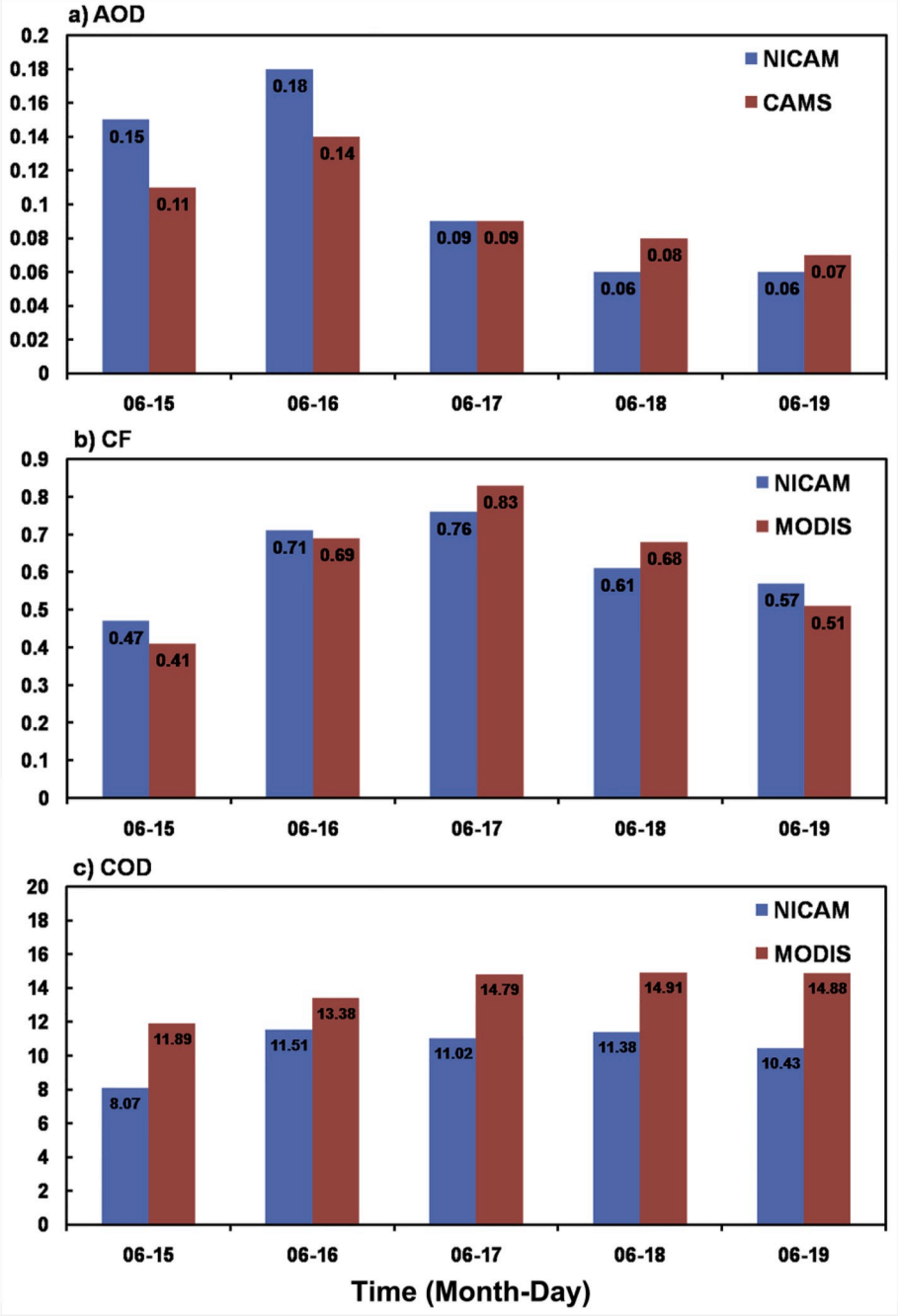

Fig. 5. Daily mean (a) AOD from CAMS product and NICAM simulations, (b) cloud fraction and (c) cloud optical depth from MODIS observations and NICAM simulations over the TP during 15–19 July 2016.

2008a). This scheme can simulate the convective systems, so no cumulus parameterization is used (Tomita, 2008a; Roh and Satoh, 2014; Goto et al., 2017). Besides, the indirect effect of the aerosols is switched on.

The 6-h Final Analysis (FNL) dataset from National Centers for Environmental Prediction (NCEP) is used for the initial conditions, the simulated results are output at half-hour intervals from 12:00 UTC on 14 July to 23: 00 UTC on July 19, 2016, and the first 12 h are used for the spin-up. More details about NICAM and SPRINTARS models can be obtained from Goto et al. (2011a, 2011b, 2012 and 2015b), Niwa et al. (2011a, 2011b), Tomita (2008b) and Uchida et al. (2016).

To verify and quantify the impact of Taklimakan dust on the cloud properties and precipitation, we carried out a control simulation (C_SIM) and a sensitivity simulation (S_SIM) in this study. In the C_SIM experiment, all kinds of aerosols in the study area were taken into account. In the S_SIM experiment, the dust aerosols emitted in the Taklimakan desert were removed by setting the dust emission factor in region 6 (Fig. 1b) as zero. The difference between C_SIM and S_SIM experiments can be considered as the contribution of Taklimakan dusts.

4. Model evaluation

Fig. 1a shows the study area containing the TP covering the region of 25–40°N, 74–104°E. The purple and red lines in Fig. 1a indicate the main areas of the TP derived from NICAM simulation and geophysical data of the National Oceanic and Atmospheric Administration (NOAA), respectively. Comparison shows that NICAM can almost exactly figure out the topography of the TP. The geophysical data can be obtained from the website: (https://www.ngdc.noaa.gov/mgg/global/relief/ETOPO2

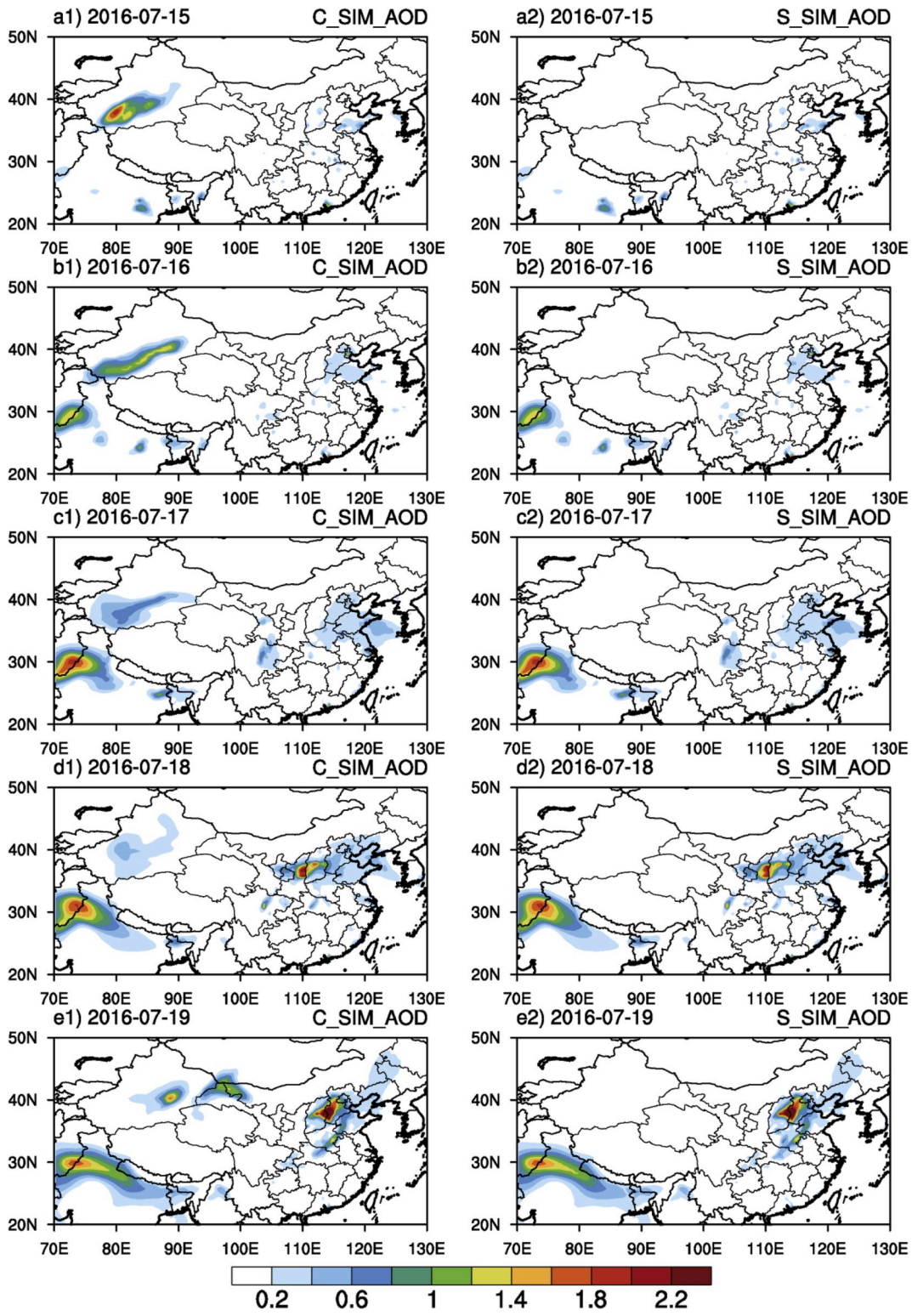

Fig. 6. Distributions of daily mean AOD simulated by NICAM during 15–19 July 2016. (a1-e1) from C_SIM experiment and (a2-e2) for S_SIM experiment.

/ETOPO2v2-2006/ETOPO2v2g/netCDF/).

Focusing on an observed event (15–19 July 2016) of Taklimakan dust lifting and affecting convective clouds over the TP and downstream rainfall (Liu et al., 2019a), we performed the simulations to verify the contribution of Taklimakan dust and investigate the mechanisms. The control simulation (C_SIM) is conducted by including all kinds of aerosols in the model. Fig. 2 shows the comparison of spatial distributions of daily mean AOD at 550 nm derived from MODIS (left column) observation, CAMS product (middle column) and simulations under C_SIM experiment by NICAM (right column) from 15 July to July 19, 2016. Due to the influence of cloud cover, MODIS missed some observations of AOD (Fig. 2 a1-e1) during this period. However, the high-AOD areas over Taklimakan desert and Thar desert were detected by MODIS. The CAMS product also shows high values of AOD in Taklimakan desert and Thar desert. In addition, the product shows there exist high AODs in North China (Fig. 2 a2-e2), which were not detected by satellite due to

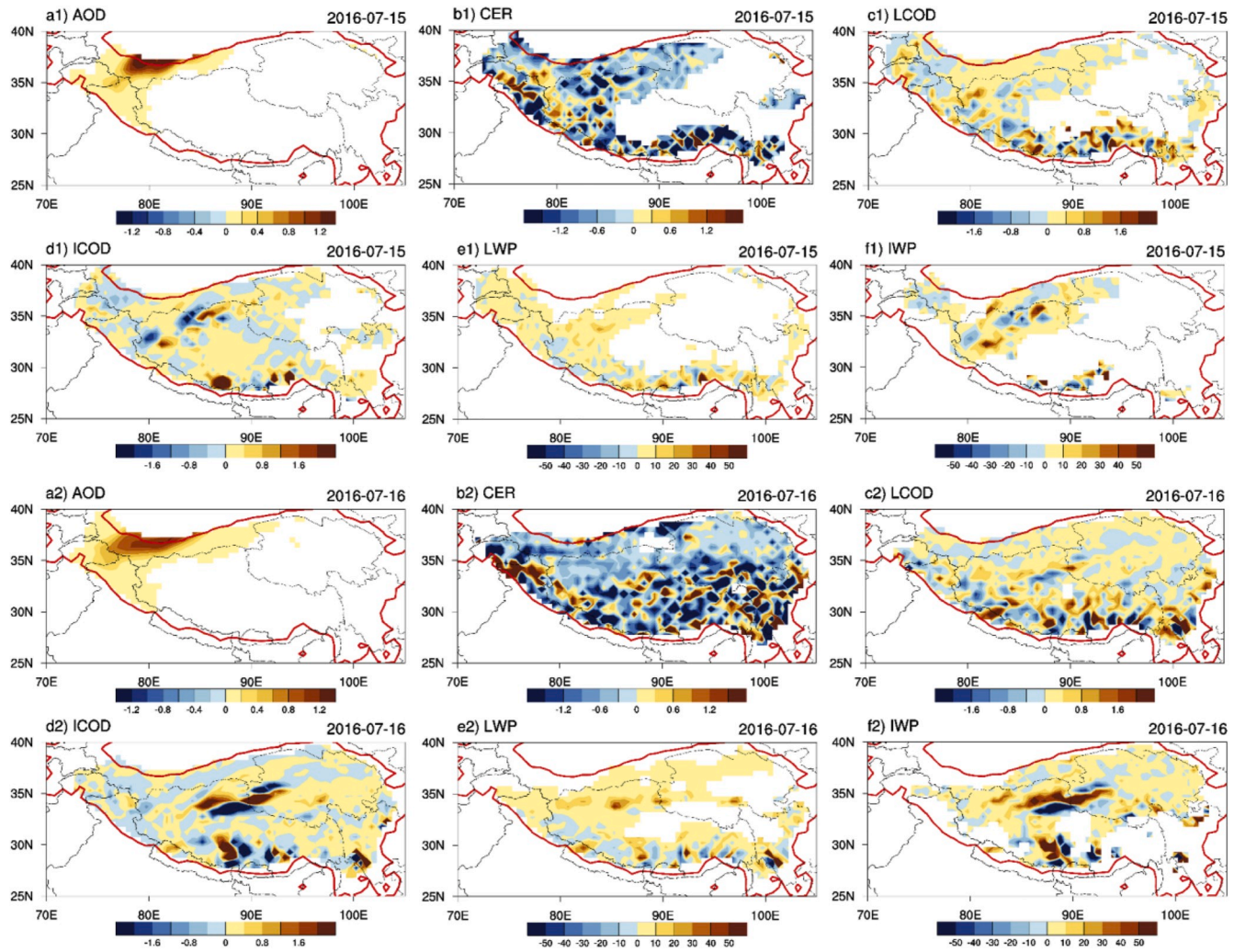

Fig. 7. Distributions of daily mean differences of (a1-a2) aerosol optical depth, (b1-b2) cloud particle effective radius, (c1-c2) liquid cloud optical depth, (d1-d2) ice cloud optical depth, (e1-e2) liquid water path and (f1-f2) ice water path from C_SIM and S_SIM simulations on 15 July and July 16, 2016. The red lines indicate the main area of the TP. (For interpretation of the references to colour in this figure legend, the reader is referred to the Web version of this article.)

cloud cover. Consistent with CAMS product, the C_SIM experiment by NICAM show high values of AOD over Taklimakan desert, Thar desert and North China (Fig. 2 a3-e3). In CAMS and NICAM, the aerosol types are divided into five categories: organic carbon (OC), black carbon (BC), sulfate, sea salt and dust. NICAM simulations and CAMS products show that the aerosols in Taklimakan desert and Thar desert are dust aerosols, and those in North China are sulfate aerosols during the event from 15 to 19 July 2016 (Figures omitted). Overall, the simulated AODs by NICAM are considered to be relative accurate based on the comparisons with satellite observations and reanalysis data.

Fig. 3 gives the distributions of daily mean CF derived from MODIS observations and simulated under C_SIM experiment by NICAM. As shown in Fig. 3, the spatial distributions of daily mean CF simulated under C_SIM experiment (Fig. 3a2-e2) are consistent with those from the MODIS product (Fig. 3a1-e1). Especially, over North India, South and North China and the TP, the simulations by NICAM are in good agreement with the satellite observations. During 17–19 July 2016, the CFs simulated by NICAM over Xinjiang province in China and the areas in Mongolia are slightly smaller than those observed by MODIS. In general, NICAM can represent the spatial distribution of CF over study area. Similar to the simulations of CF, the spatial distributions of the COD under C_SIM experiment (Fig. 4a2-e2) are in good agreement with those derived from satellite observations (Fig. 4a1-e1) in North India, North China and the TP.

To give a quantitative evaluation for the model simulation, the regional average AOD, CF and COD over the TP are further calculated and compared with the observations and reanalysis data. Fig. 5 presents the comparisons of daily mean AOD and cloud properties from the simulations under C_SIM experiment over the TP during 15–19 July 2016. As shown in Fig. 5a and b, it indicates that, besides giving reasonable patterns (Figs. 2 and 3), NICAM can quantify well the values of AOD and CF. In addition, although NICAM underestimates the COD in some degree, the mean deviation of simulation by NICAM from MODIS observation is below 25% (the maximum is 29.9% on 19 July). Therefore, NICAM is overall deemed reliable for investigating the values and distributions of AOD and cloud properties in the study area. Moreover, although there are some deviations in the cloud properties of the simulations for high latitudes, such as Xinjiang province of China and Mongolia, it does not affect the main conclusion of this study because satellite observations indicate clouds over these regions have no contribution to downstream precipitation (Liu et al., 2019a).

5. Impacts of Taklimakan dust on northern rainfall

In the previous study based on observations for the same event by Liu et al. (2019a), it was found that the dust aerosols originating from the Taklimakan desert can be lifted to the TP and consequently affects the convective clouds over the TP during 15–19 July 2016. The continuous

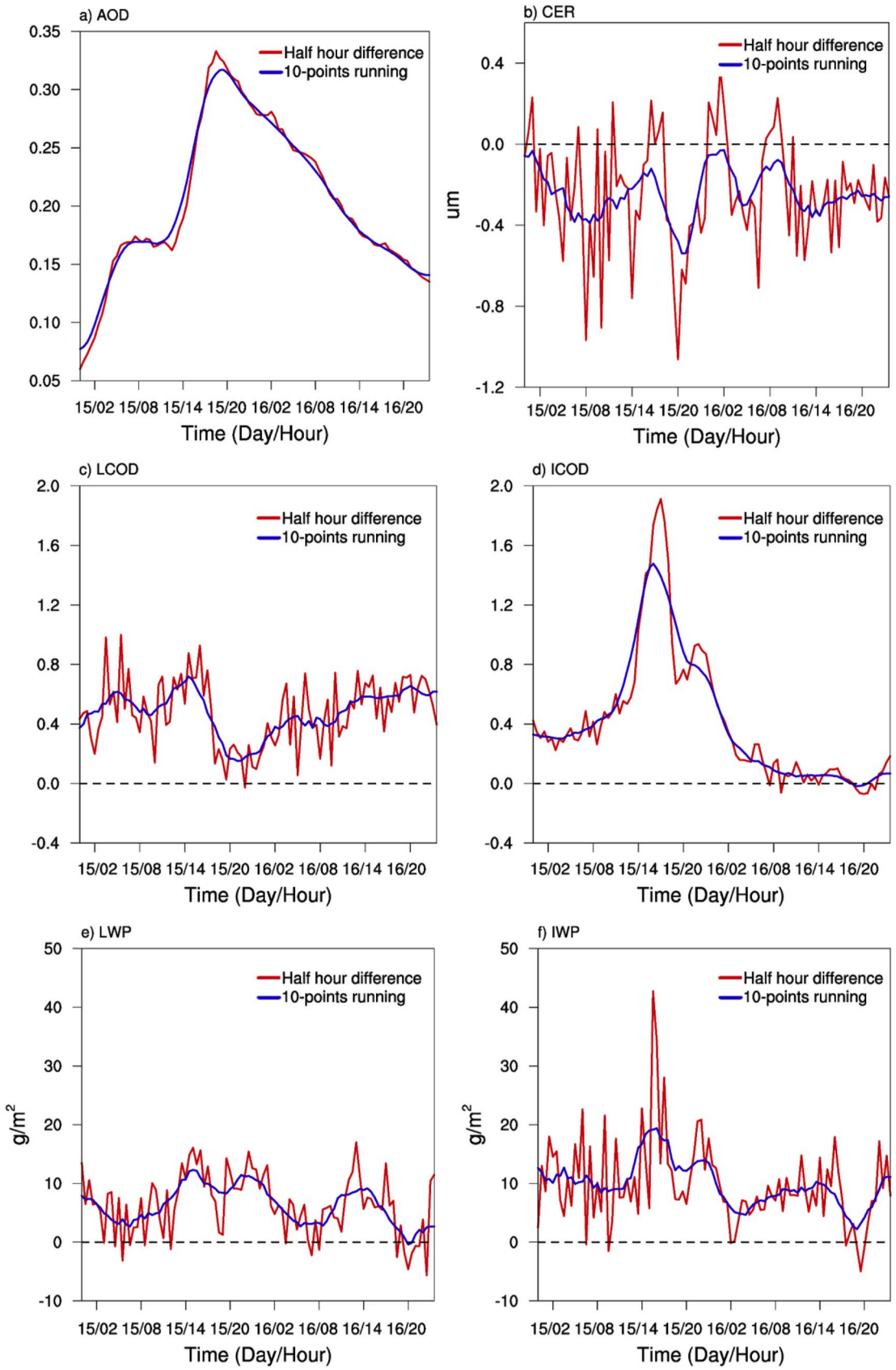

Fig. 8. Time series of every-half-hour differences (red lines) of (a) aerosol optical depth, (b) cloud particle effective radius, (c) liquid cloud optical depth, (d) ice cloud optical depth, (e) liquid water path and (f) ice water path from C_SIM and S_SIM simulations over the TP during 15–16 July 2016. The blue lines indicate the value of 10-points running average. (For interpretation of the references to colour in this figure legend, the reader is referred to the Web version of this article.)

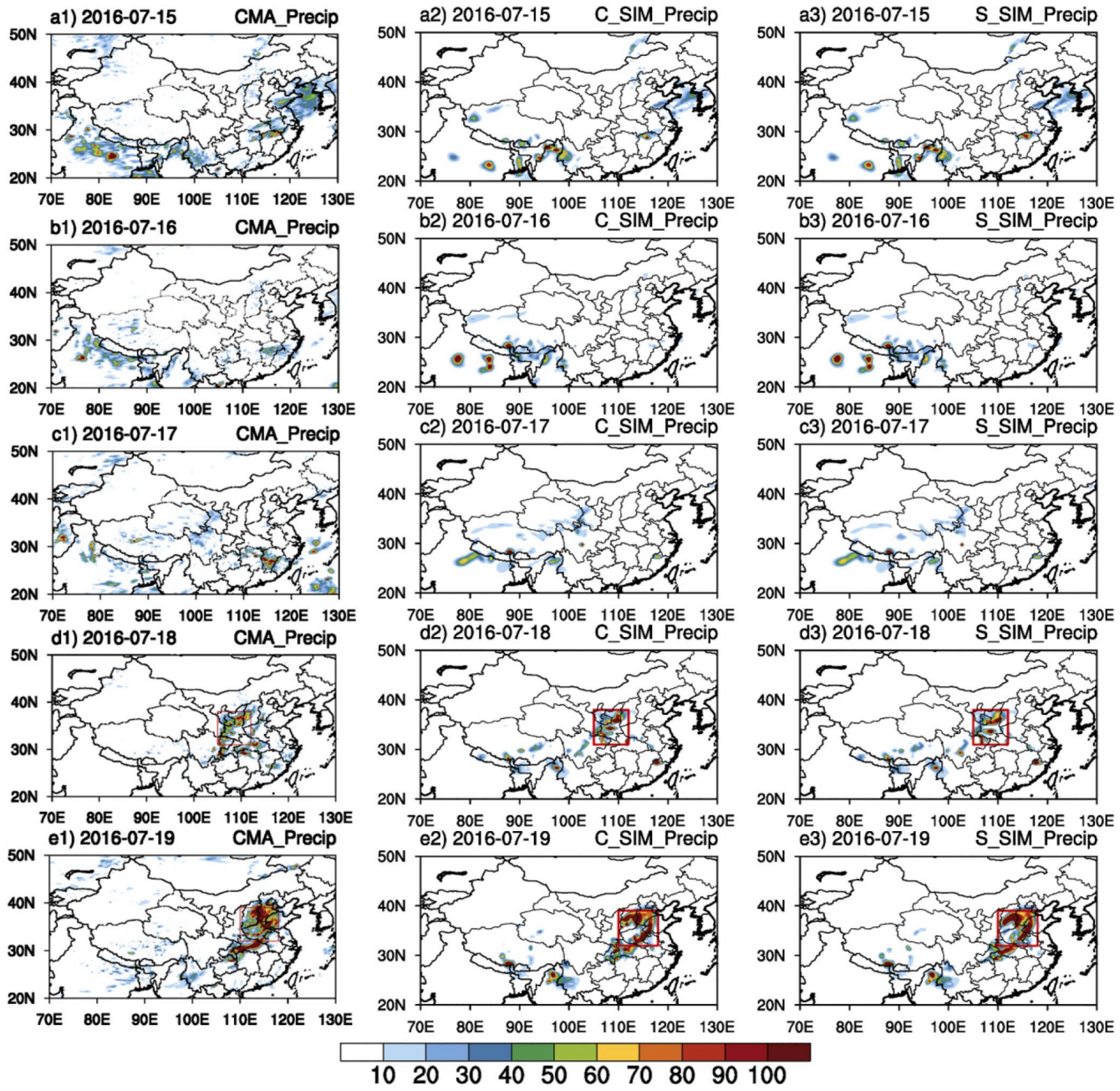

Fig. 9. Distribution of daily cumulative rainfall (unit: mm) derived from (a1-e1) CMA reanalysis data, (a2-e2) C_SIM and (a3-e3) S_SIM simulations during 15–19 July 2016.

eastward movement of dust-polluted convective clouds from the TP could trigger the heavy rainfall over North China and the Yangtze River basin. To verify this process, the S_SIM experiment is carried out and compared with the simulation under C_SIM experiment to reveal the role of Taklimakan dusts in this event.

Fig. 6 presents the distributions of simulated AOD under C_SIM and S_SIM experiments by NICAM. The difference between C_SIM and S_SIM experiments is evident from Fig. 6 across the Taklimakan desert region as the dust emissions are removed over there in S_SIM experiment. Furthermore, Fig. 7 shows the difference (C_SIM minus S_SIM) of AOD (Fig. 7a1 and a2) and responses of cloud properties, including cloud particle effective radius (CER) (Fig. 7b1 and b2), liquid cloud optical depth (LCOD) (Fig. 7c1 and c2), ice cloud optical depth (ICOD) (Fig. 7d1 and d2), liquid water path (LWP) (Fig. 7e1 and e2) and ice water path (IWP) (Fig. 7f1 and f2), due to the dust aerosols from the Taklimakan desert on 15 July and July 16, 2016.

On July 15, 2016, there are small amounts of dust aerosols over the northern slope of the TP (Fig. 7a1), and the CER over the northern TP becomes smaller (Fig. 7b1), which indicates that these dust aerosols can affect the development of clouds by acting as cloud condensation nuclei and ice nuclei (Huang et al., 2006b; Wang et al., 2010). Correspondingly, due to the reduction of particle radius, the cloud albedo is enhanced, resulting in an increased COD (Fig. 7c1 and d1); meanwhile, more cloud condensation nuclei and ice nuclei increase water content in the clouds (Fig. 7e1 and f1) (Koch and Genio, 2010; Saito and Hayasaka, 2014). With the movement and development of the clouds, they cover the entire TP, and the impacts of dust aerosols on clouds still exist on July 16, 2016 (Fig. 7b2-f2).

Fig. 8 shows the half hour time series of differences of dust AOD and cloud properties between the results under C_SIM and S_SIM

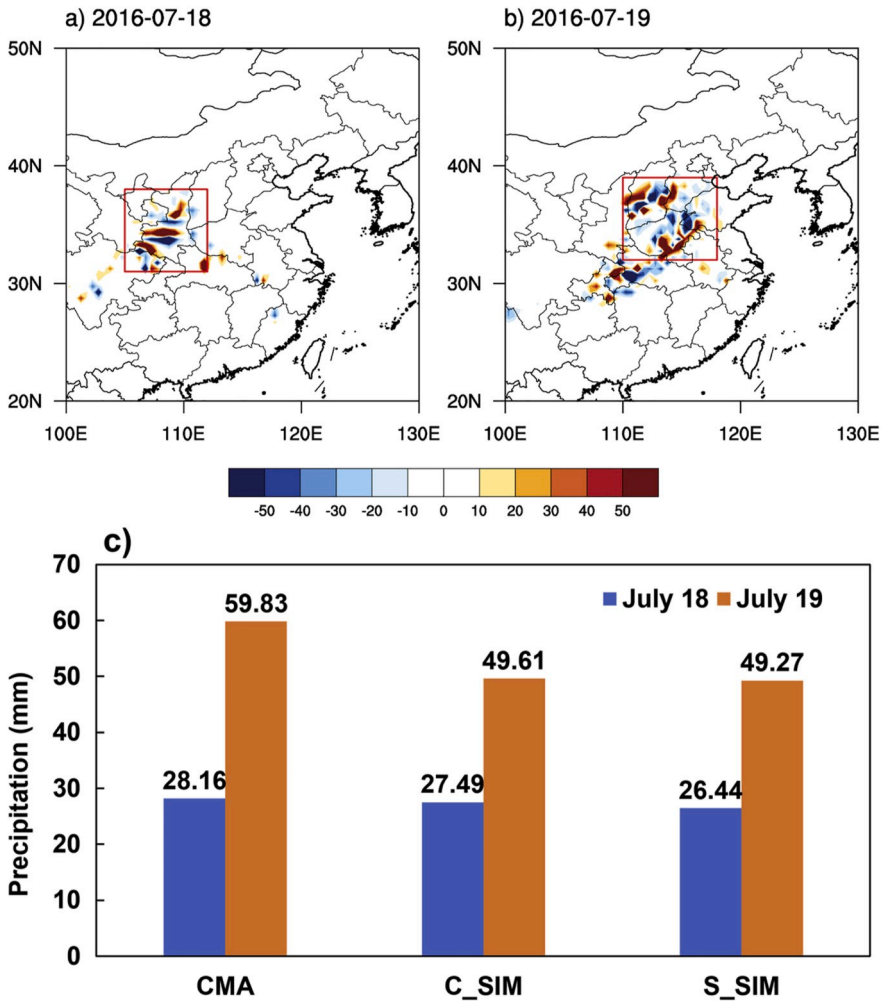

Fig. 10. Distributions of daily mean differences of precipitation simulated by C_SIM and S_SIM experiments on (a) 18 July, (b) July 19, 2016 from observations, and (c) the regional average (red rectangles) of daily cumulative rainfall obtained from observations and NICAM simulations. (For interpretation of the references to colour in this figure legend, the reader is referred to the Web version of this article.)

experiments over the TP from 15 to 16 July 2016. The results indicate that the AOD gradually increased and peaked with a value of 0.33 at 19:00 UTC on 15 July and then gradually decreased (Fig. 8a). Corresponding to the change in dust aerosols, the CER over the TP reached a maximum at 20:30 UTC on 15 July (Fig. 8b); the LCOD, ICOD, LWP and IWP all increased initially and then decreased gradually after reaching their peak values (Fig. 8c–f). The change of each cloud parameter is consistent with the change of dust AOD. Comparing the responses of ice cloud properties (ICOD and IWP) and liquid cloud properties (LCOD and LWP), it is observed that the responses of ice clouds to dust aerosols are more obvious, which is consistent with our previous study through satellite observations (Liu et al., 2019a), especially the maximum response of ICOD and IWP can reach to 1.91 and 42.74 g/m^2, respectively. A series of changes in dust aerosols and cloud properties suggest that the dust aerosols can promote the development of clouds mainly through indirect effect after they are lifted to the TP, which can also prolong cloud lifetime (Myhre et al., 2007; Rosenfeld et al., 2008). According to previous studies (Rosenfeld et al., 2008; Guo et al., 2016, 2017; 2019; Lee et al., 2016; Jiang et al., 2018; Wang et al., 2018), under the conditions of lower aerosol loading (0 < AOD < ~0.3), the direct and semi-direct effects of aerosols are weak in altering cloud properties, while the indirect effect on clouds is significant and dominant. In this study, the indirect effect of the aerosols is included in simulations. Thus, based on the range of AOD values (0 < AOD < 0.33) and the response of cloud properties to dust aerosols, it can be determined that aerosols affected clouds mainly through the indirect effect during this event.

Furthermore, to reliably extract the influence of dust-polluted clouds on the downstream rainfall, we firstly compared the simulated rainfall (Fig. 9a2-e2 and a3-e3) with the observations (Fig. 9a1-e1). On the whole, the C_SIM (Fig. 9a2-e2) and S_SIM (Fig. 9a3-e3) experiments in NICAM can accurately capture the location and intensity of the rainfall during this event. On 15 July (Fig. 9a1-a3), the NICAM can capture the rainfall over North India, the TP and Eastern China to the Korean peninsula. On 16 and 17 July, the NICAM still has a great performance for precipitation simulation over the TP and North India except Southeast China (Fig. 9b1-b3 and c1-c3). On 18 and 19 July, the rainfall over Central China and North China is successfully simulated by NICAM (Fig. 9d1-d3 and e1-e3).

Fig. 10a and b presents the difference of daily cumulative precipitation between the C_SIM and S_SIM experiments over the north area (red rectangles in Fig. 9) on 18 and July 19, 2016. Due to the changes in cloud properties, the location of rainfall has changed. Fig. 10c shows the regional averaged daily cumulative precipitation over the north area obtained by CMA observations and NICAM simulations. As indicated in Fig. 10c, the C_SIM can effectively capture the precipitation on 18 July. However, for 19 July, there are some deviations between the simulations and the observations, mainly because the coverage of rainfall simulated by NICAM is relatively small (Fig. 9e1-e3). According to the classification of rainfall level by CMA, the observed and simulated rainfall have reached the level of heavy rain (rainfall>25 mm/day) on

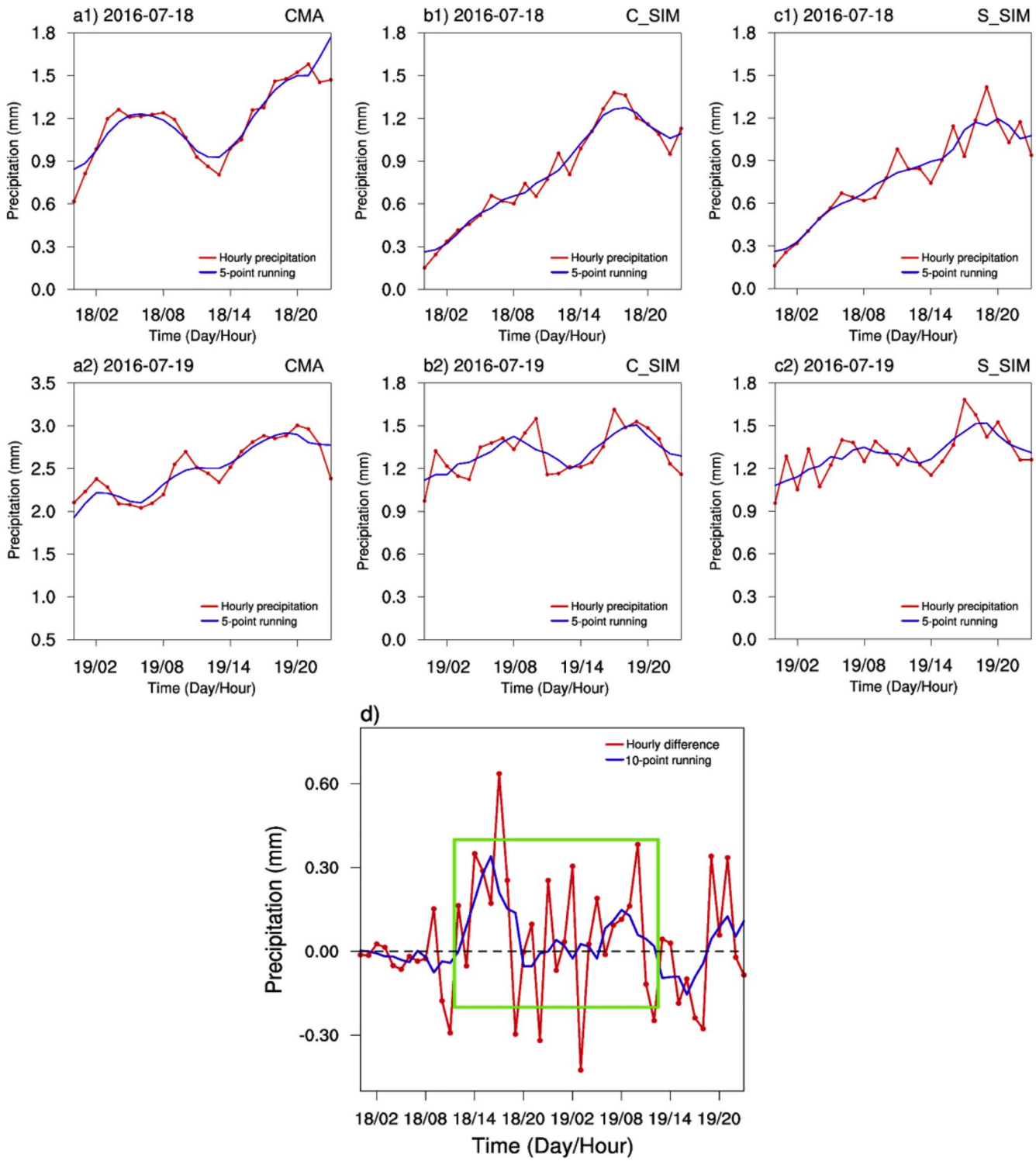

Fig. 11. Time series of hourly precipitation (red lines) derived from (a1-a2) CMA and simulated by (b1-b2) C_SIM and (c1-c2) S_SIM experiments on 18 July and July 19, 2016. (d) Hourly differences of simulated rainfall by C_SIM and S_SIM experiments. (For interpretation of the references to colour in this figure legend, the reader is referred to the Web version of this article.)

18 and 19 July. Comparing the rainfall simulated by C_SIM with that by S_SIM, it can be found that when the Taklimakan dusts are considered in the NICAM, the simulations are closer to the observations. Additionally, comparison of the results from C_SIM and S_SIM simulations indicates that the rainfall simulated by the experiment containing Taklimakan dusts is greater than that free of Taklimakan dusts both on 18 and 19 July (Fig. 10c).

Based on hourly regional averaged precipitation of north area, a more detailed analysis of precipitation simulated by C_SIM and S_SIM on 18 and July 19, 2016 are performed (as shown in Fig. 11). Though the observed heavy rain from 03:00 to 09:00 UTC on July 18, 2016 over north area (Fig. 11a1) is not successfully simulated by C_SIM and S_SIM, both experiments have captured the gradually increase in precipitation after 13:00 UTC on18 July 2016 (Fig. 11a1-c1). Relatively, compared

with S_SIM, C_SIM experiment can better figure out the gradual increase in precipitation and more heavy rain after 13:00 on 18 July (Fig. 11b1-c1). For the precipitation on the July 19, 2016, both experiments can capture the time variation of precipitation, but there is an underestimation for the rainfall intensity (Fig. 11a2-c2). Compared with the observations, C_SIM can capture the peak precipitation well at 10:00 UTC on19 July 2016 (Fig. 11a2 and b2). Similarly, the C_SIM performs better in capturing the increase in precipitation and the continued heavy rain after 13:00 on 19 July. The hourly differences of precipitation from C_SIM and S_SIM are shown in Fig. 10d, which indicates that the impacts of aerosols on clouds can change the spatial and temporal distribution of precipitation over downstream region. The rainfall intensity decreased in the first 12 h (00:00 to 11:00 UTC on 18 July) and showed a significant increase during the next 25 h (12:00 UTC on 18 July to 12:00 UTC on 19 July, green rectangle in Fig. 11d), especially during 12:00 to 20:00 UTC on 18 July and 04:00 to 14:00 UTC on19 July. The maximum value of precipitation variation can reach to 0.64 mm/h. The change of precipitation shows that dust aerosols can promote the development of clouds, delay the occurrence of heavy rainfall and increase the intensity of precipitation.

6. Conclusions and discussions

In this study, using an aerosol-coupled model, the impacts of Taklimakan dusts on the cloud properties over the TP and downstream precipitation are investigated. Dust aerosols over the TP can reduce the CER and increase ICOD and IWP. The dust aerosols promoted the development of clouds and prolonged cloud lifetime; correspondingly, influenced the downstream precipitation. The developed clouds enhanced the intensity of heavy rainfall and delayed the occurrence of heavy rainfall over north area, which is similar to the conclusion that aerosols have an invigoration effect on heavy rain (Petters et al., 2006; Rosenfeld et al., 2008). Therefore, when the dust aerosols originating from the Taklimakan desert reach the TP, it could affect the downstream precipitation by affecting the cloud properties. Meanwhile, the spatial distribution of dust aerosols simulated by NICAM indicates that no dust aerosols appeared in the downstream region, so it can be concluded that no dust aerosols are directly transported from the Taklimakan desert to the downstream. Thus, in this case study, the downstream precipitation is dominantly influenced by the Taklimakan-dusts-polluted clouds outflowing from the TP instead of local dust aerosols along the clouds moving path.

In the previous study, the evidence of aerosols affecting clouds over the TP and influencing downstream precipitation was observed by satellites. Although the effect of aerosols on cloud properties and precipitation is quantified in this study, there is still some uncertainty in the model: the resolution of the mode is about 7 km which may be the reason why the precipitation in Southeast China is not successfully simulated (Fig. 9c1-c3). In the future, upon improving the computing resources, a higher-resolution simulation will be performed. Meanwhile, although the deviations in the cloud properties of the simulations for high latitudes have no impact on the main conclusions in this case study, the model still needs further optimization.

On the whole, this study demonstrates the mechanism of Taklimakan dust effects on cloud properties over the TP and downstream rainfall, which may provide a new perspective to study the impact of the TP on the surrounding droughts.

Declaration of competing interest

The authors declare that they have no known competing financial interests or personal relationships that could have appeared to influence the work reported in this paper.

Acknowledgements

This research was mainly supported by the Strategic Priority Research Program of the Chinese Academy of Sciences (Grant No. XDA2006010301), and jointly supported by the National Natural Science Foundation of China (91737101, 91937302, 41991231, 91744311) and the Fundamental Research Funds for the Central Universities (lzujbky-2019-kb30). We are grateful to the model developers of SPRINTARS (https://sprintars.riam.kyushu-u.ac.jp/indexe.html) and NICAM (http://nicam.jp/).

Appendix A. Supplementary data

Supplementary data to this article can be found online at https://doi.org/10.1016/j.atmosenv.2020.117583.

References

Joyce, R.J., Janowiak, J.E., Arkin, P.A., Xie, P., 2004. CMORPH: a method that produces global precipitation estimates from passive microwave and infrared data at high spatial and temporal resolution. J. Hydrometeorol. 5 (3), 487–503. https://doi.org/10.1175/1525-7541(2004)005<0487:camtpg>2.0.co;2.

Takemura, T., Nakajima, T., Dubovik, O., Holben, B.N., Kinne, S., 2002. Single-scattering albedo and radiative forcing of various aerosol species with a global three-dimensional model. J. Clim. 15, 333–352. https://doi.org/10.1175/1520-0442(2002)015<0333:SSAARF>2.0.CO;2.

Ackerman, A.S., Toon, O.B., Stevens, D.E., Heymsfield, A.J., Ramanathan, V., Welton, E. J., 2000. Reduction of tropical cloudiness by soot. Science 288, 1042–1047. https://doi.org/10.1126/science.288.5468.1042.

Albrecht, B.A., 1989. Aerosols, cloud microphysics, and fractional cloudiness. Science 245, 1227–1230. https://doi.org/10.1126/science.245.4923.1227.

Andreae, M.Q., Rosenfeld, D., Artaxo, P., Costa, A.A., Frank, G.P., Longo, K.M., Silva-Dias, M., 2004. Smoking rain clouds over the Amazon. Science 303, 1337–1342. https://doi.org/10.1126/science.1092779.

Benedetti, A., Morcrette, J.J., Boucher, O., Dethof, A., Engelen, R., Fisher, M., Flentje, H., Huneeus, N., Jones, L., Kaiser, J.W., Kinne, S., Mangold, A., Razinger, M., Simmons, A.J., Suttie, M., 2009. Aerosol analysis and forecast in the European center for medium-range weather forecasts integrated forecast system: 2. Data assimilation. J. Geophys. Res. Atmos. 114 (D6), 605–617. https://doi.org/10.1029/2008JD011115.

Dai, T., Goto, D., Schutgens, N.A.J., Dong, X., Nakajima, T., 2014a. Simulated aerosol key optical properties over global scale using an aerosol transport model coupled with a new type of dynamic core. Atmos. Environ. 82 (1), 71–82. https://doi.org/10.1016/j.atmosenv.2013.10.018.

Dai, T., Schutgens, N.A.J., Goto, D., Shi, G., Nakajima, T., 2014b. Improvement of aerosol optical properties modeling over eastern Asia with MODIS AOD assimilation in a global non-hydrostatic icosahedral aerosol transport model. Environ. Pollut. 195, 319–329. https://doi.org/10.1016/j.envpol.2014.06.021.

Dai, T., Shi, G., Nakajima, T., 2015. Analysis and evaluation of the global aerosol optical properties simulated by an online aerosol-coupled non-hydrostatic icosahedral atmospheric model. Adv. Atmos. Sci. 32 (6), 743–758. https://doi.org/10.1007/s00376-014-4098-z.

Dai, T., Cheng, Y.M., Zhang, P., Shia, G.Y., Sekiguchi, M., Suzuki, K., Goto, D., Nakajima, T., 2018. Impacts of meteorological nudging on the global dust cycle simulated by NICAM coupled with an aerosol model. Atmos. Environ. 190, 99–115. https://doi.org/10.1016/j.atmosenv.2018.07.016.

Fan, J., Leung, L.R., DeMott, P.J., Comstock, J.M., Singh, B., Rosenfeld, D., Tomlinson, J. M., White, A., Prather, K.A., Minnis, P., Ayers, J.K., Min, Q., 2014. Aerosol impacts on California winter clouds and precipitation during CalWater 2011: local pollution versus long-range transported dust. Atmos. Chem. Phys. 14, 81–101. https://doi.org/10.5194/acp-14-81-2014.

Fan, J., Rosenfeld, D., Yang, Y., Zhao, C., Leung, L.R., Li, Z., 2015. Substantial contribution of anthropogenic air pollution to catastrophic floods in Southwest China. Geophys. Res. Lett. 42 (14), 6066–6075. https://doi.org/10.1002/2015GL064479.

Fan, J., Zhang, R., Tao, W.K., Mohr, K., 2008. Effects of aerosol optical properties on deep convective clouds and radiative forcing. J. Geophys. Res. Atmos. 113 https://doi.org/10.1029/2007jd009257. D08, 209.

Fan, H., Zhao, C., Yang, Y.K., 2020. A comprehensive analysis of the spatio-temporal variation of urban air pollution in China during 2014-2018. Atmos. Environ. 220 https://doi.org/10.1016/j.atmosenv.2019.117066.

Feingold, G., Jiang, H., Harrington, J.Y., 2005. On smoke suppression of clouds in Amazonia. Geophys. Res. Lett. 32, L02804. https://doi.org/10.1029/2004GL021369.

Garrett, T.J., Zhao, C., 2006. Increased arctic cloud longwave emissivity associated with pollution from mid-latitudes. Nature 440 (7085), 787–789. https://doi.org/10.1038/nature04636.

Goto, D., Nakajima, T., Takemura, T., Sudo, K., 2011a. A study of uncertainties in the sulfate distribution and its radiative forcing associated with sulfur chemistry in a global aerosol model. Atmos. Chem. Phys. 11 (21), 10889–10910. https://doi.org/10.5194/acpd-11-12269-2011.

Goto, D., Schutgens, N.A.J., Nakajima, T., Takemura, T., 2011b. Sensitivity of aerosol to assumed optical properties over Asia using a global aerosol model and AERONET. Geophys. Res. Lett. 38 (17), L17810. https://doi.org/10.1029/2011GL048675.

Goto, D., Kanazawa, S., Nakajima, T., Takemura, T., 2012. Evaluation of a relationship between aerosols and surface downward shortwave flux through an integrative analysis of modeling and observation. Atmos. Environ. 49, 294–301. https://doi.org/10.1016/j.atmosenv.2011.11.032.

Goto, D., Dai, T., Satoh, M., Tomita, H., Uchida, J., Misawa, S., Inoue, T., Tsuruta, H., Ueda, K., Ng, C.F.S., Takami, A., Sugimoto, N., Shimizu, A., Ohara, T., Nakajima, T., 2015a. Application of a global no hydrostatic model with a stretched-grid system to regional aerosol simulations around Japan. Geosci. Model Dev. (GMD) 8, 235–259. https://doi.org/10.5194/gmd-8-235-2015.

Goto, D., Nakajima, T., Dai, T., Takemura, T., Kajino, M., Matsui, H., Takami, A., Hatakeyama, S., Sugimoto, N., Shimizu, A., Ohara, T., 2015b. An evaluation of simulated particulate sulfate over East Asia through global model intercomparison. J. Geophys. Res. Atmos. 120 (12), 6247–6270. https://doi.org/10.1002/2014JD021693.

Goto, D., Sato, Y., Yashiro, H., Suzuki, K., Nakajima, T., 2017. Validation of high-resolution aerosol optical thickness simulated by a global non-hydrostatic model against remote sensing measurements. Radiation Processes in the Atmosphere & Ocean 1810, 1000021–1000024. https://doi.org/10.1063/1.4975557.

Guo, J., Deng, M., Fan, J., Li, Z., Chen, Q., Zhai, P., Dai, Z., Li, X., 2014. Precipitation and air pollution at mountain and plain stations in northern China: insights gained from observations and modeling. J. Geophys. Res. Atmos. 119, 4793–4807. https://doi.org/10.1002/2013JD021161.

Guo, J., Deng, M., Lee, S.S., Wang, F., Li, Z., Zhai, P., Liu, H., Lv, W., Yao, W., Li, X., 2016. Delaying precipitation and lightning by air pollution over the Pearl River delta. Part I: observational analyses. J. Geophys. Res. Atmos. 121 (11), 6472–6488. https://doi.org/10.1002/2015JD023257.

Guo, J., Su, T., Li, Z., Miao, Y., Li, J., Liu, H., Xu, H., Cribb, M., Zhai, P., 2017. Declining frequency of summertime local-scale precipitation over eastern China from 1970 to 2010 and its potential link to aerosols. Geophys. Res. Lett. 44 (11), 5700–5708. https://doi.org/10.1002/2017GL073533.

Guo, J., Su, T., Chen, D., Wang, J., Li, Z., Lv, Y., Guo, X., Liu, H., Cribb, M., Zhai, P., 2019. Declining summertime local-scale precipitation frequency over China and the United States, 1981-2012: the disparate roles of aerosols. Geophys. Res. Lett. 46 (22), 13281–13289. https://doi.org/10.1029/2019GL085442.

Huang, J., Lin, B., Minnis, P., Wang, T., Wang, X., Hu, Y., Yi, Y., Ayers, J., 2006a. Satellite-based assessment of possible dust aerosols semi-direct effect on cloud water path over East Asia. Geophys. Res. Lett. 33, L19802. https://doi.org/10.1029/2006GL026561.

Huang, J.P., Minnis, P., Lin, B., Wang, T., Yi, Y., Hu, Y., Sun-Mack, S., Ayers, K., 2006b. Possible influences of Asian dust aerosols on cloud properties and radiative forcing observed from MODIS and CERES. Geophys. Res. Lett. 33, L06824. https://doi.org/10.1029/2005GL024724.

Huang, J., Minnis, P., Yi, Y.H, Tang, Q., Wang, X., Hu, Y., Liu, Z., Ayers, K., Trepte, C., Winker, D., 2007. Summer dust aerosols detected from CALIPSO over the Tibetan Plateau. Geophys. Res. Lett. 34 https://doi.org/10.1029/2007GL029938.

Huang, J., Fu, Q., Su, J., Tang, Q., Minnis, P., Hu, Y., Yi, Y., Zhao, Q., 2009. Taklimakan dust aerosol radiative heating derived from CALIPSO observations using the Fu-Liou radiation model with CERES constraints. Atmos. Chem. Phys. 9 (12), 4011–4021. https://doi.org/10.5194/acp-9-4011-2009.

Huang, J.P., Minnis, P., Yan, H., Yi, Y., Chen, B., Zhang, L., Ayers, J.K., 2010. Dust aerosol effect on semi-arid climate over Northwest China detected from A-Train satellite measurements. Atmos. Chem. Phys. 10, 6863–6872. https://doi.org/10.5194/acp-10-6863-2010.

Huang, J., Wang, T., Wang, W., Li, Z., Yan, H., 2014. Climate effects of dust aerosols over East Asian arid and semiarid regions. J. Geophys. Res. Atmos. 119 (19), 11398–11416. https://doi.org/10.1002/2014JD021796.

Jia, R., Liu, Y., Chen, B., Zhang, Z., Huang, J., 2015. Source and transportation of summer dust over the Tibetan Plateau. Atmos. Environ. 123, 210–219. https://doi.org/10.1016/j.atmosenv.2015.10.038.

Jia, R., Liu, Y.Z., Hua, S., Zhu, Q.Z., Shao, T.B., 2018. Estimation of the aerosol radiative effect over the Tibetan Plateau based on the latest CALIPSO product. J. Meteor. Res. 32 (5), 707–722. https://doi.org/10.1007/s13351-018-8060-3.

Jia, R., Luo, M., Liu, Y., Zhu, Q.Z., Hua, S., Wu, C.Q., Shao, T.B., 2019. Anthropogenic aerosol pollution over the eastern slope of the Tibetan plateau. Adv. Atmos. Sci. 36 (8), 847–862. https://doi.org/10.1007/s00376-019-8212-0.

Jiang, J.H., Su, H., Huang, L., Wang, Y., Massie, S., Zhao, B., Omar, A., Wang, Z., 2018. Contrasting effects on deep convective clouds by different types of aerosols. Nat. Commun. 9, 3874. https://doi.org/10.1038/s41467-018-06280-4.

Jin, Q., Wei, J., Yang, Z.L., 2014. Positive response of Indian summer rainfall to Middle East dust. Geophys. Res. Lett. 41, 4068–4074. https://doi.org/10.1002/2014GL059980.

Khain, A.P., BenMoshe, N., Pokrovsky, A., 2008. Factors determining the impact of aerosols on surface precipitation from clouds: an attempt at classification. J. Atmos. Sci. 65, 1721–1748. https://doi.org/10.1175/2007JAS2515.1.

Koch, D., Genio, A.D., 2010. Black carbon absorption effects on cloud cover, review and synthesis. Atmos. Chem. Phys. 10 (3), 7685–7696. https://doi.org/10.5194/acp-10-7685-2010.

Koren, I., Altaratz, O., Remer, L.A., Feingold, G., Martins, J.V., Heiblum, R.H., 2012. Aerosol-induced intensification of rain from the tropics to the mid-latitudes. Nat. Geosci. 5, 118–122. https://doi.org/10.1038/ngeo1364.

Kuhlmann, J., Quaas, J., 2010. How can aerosols affect the Asian summer monsoon? Assessment during three consecutive pre-monsoon seasons from CALIPSO satellite data. Atmos. Chem. Phys. 10, 4673–4688. https://doi.org/10.5194/acp-10-4673-2010.

Lamarque, J.F., Bond, T.C., Eyring, V., Granier, C., Heil, A., Klimont, Z., Lee, D., Liousse, C., Mieville, A., Owen, B., Schultz, M.G., Shindell, D., Smith, S.J., Stehfest, E., VanAardenne, J., Cooper, O.R., Kainuma, M., Mahowald, N., McConnell, J.R., Naik, V., Riahi, K., van Vuuren, D.P., 2010. Historical (1850–2000) gridded anthropogenic and biomass burning emissions of reactive gases and aerosols: methodology and application. Atmos. Chem. Phys. 10, 7017–7039. https://doi.org/10.5194/acp-10-7017-2010.

Lau, K.M., Kim, M.K., Kim, K.M., 2006. Asian summer monsoon anomalies induced by aerosol direct forcing: the role of the Tibetan Plateau. Clim. Dynam. 26, 855–864. https://doi.org/10.1007/s00382-006-0114-z.

Lau, W.K.M., Kim, M.K., Kim, K.M., Lee, W.S., 2010. Enhanced surface warming and accelerated snow melt in the Himalayas and Tibetan Plateau induced by absorbing aerosols. Environ. Res. Lett. 5 (2), 025204 https://doi.org/10.1088/1748-9326/5/2/025204.

Lee, S.S., Guo, J., Li, Z., 2016. Delaying precipitation by air pollution over the Pearl River delta: 2. model simulations. J. Geophys. Res. Atmos. 121 (19), 11739–11760. https://doi.org/10.1002/2015jd024362.

Li, Z., Niu, F., Fan, J., Liu, Y., Rosenfeld, D., Ding, Y., 2011. Long-term impacts of aerosols on the vertical development of clouds and precipitation. Nat. Geosci. 4, 888–894. https://doi.org/10.1038/ngeo1313.

Li, Z.Q., Lau, W.K.-M., Ramanathan, V., Wu, G., Ding, Y., Manoj, M.G., Liu, J., Qian, Y., Li, J., Zhou, T., Fan, J., Rosenfeld, D., Ming, Y., Wang, Y., Huang, J., Wang, B., Xu, X., Lee, S.S., Cribb, M., Zhang, F., Yang, X., Zhao, C., Takemura, T., Wang, K., Xia, X., Yin, Y., Zhang, H., Guo, J., Zhai, P.M., Sugimoto, N., Babu, S.S., Brasseur, G. P., 2016. Aerosol and monsoon climate interactions over Asia. Rev. Geophys. 54 (4), 866–929. https://doi.org/10.1002/2015RG000500.

Li, Z.Q., Wang, Y., Guo, J.P., Zhao, C.F., Cribb, M.C., Dong, X.Q., Fan, J.W., Gong, D.Y., Huang, J.P., Jiang, M.J., Jiang, Y.Q., Lee, S.S., Li, H., Li, J.M., Liu, J.J., Qian, Y., Rosenfeld, D., Shan, S.Y., Sun, Y.L., Wang, H.J., Xin, J.Y., Yan, X., Yang, X., Yang, X. Q., Zhang, F., Zheng, Y.T., 2019. East asian study of tropospheric aerosols and their impact on regional clouds, precipitation, and climate (EAST-AIR (CPC)). J. Geophys. Res. Atmos. 124 (23), 13026–13054. https://doi.org/10.1029/2019JD030758.

Liu, Y., Huang, J., Shi, G., Takamura, T., Khatri, P., Bi, J., Shi, J., Wang, T., Wang, X., Zhang, B., 2011. Aerosol optical properties and radiative effect determined from sky-radiometer over Loess Plateau of Northwest China. Atmos. Chem. Phys. 11, 11455–11463. https://doi.org/10.5194/acp-11-11455-2011, 2011.

Liu, Y., Jia, R., Dai, T., Xie, Y., Shi, G., 2014. A review of aerosol optical properties and radiative effects. J. Meteor. Res. 28 (6), 1003–1028. https://doi.org/10.1007/s13351-014-4045-z.

Liu, Y., Sato, Y., Jia, R., Xie, Y., Huang, J., Nakajima, T., 2015. Modeling study on the transport of summer dust and anthropogenic aerosols over the Tibetan Plateau. Atmos. Chem. Phys. 15 (21), 12581–12594. https://doi.org/10.5194/acpd-15-15005-2015.

Liu, Y., Zhu, Q., Huang, J., Hua, S., Jia, R., 2019a. Impact of dust-polluted convective clouds over the Tibetan Plateau on downstream precipitation. Atmos. Environ. 209, 67–77. https://doi.org/10.1016/j.atmosenv.2019.04.001.

Liu, Y., Shi, G., Xie, Y., 2013. Impact of smoke aerosol on glacial-interglacial climate. Adv. Atmos. Sci. 30 (6), 1725–1731. https://doi.org/10.1007/s00376-013-2289-7.

Liu, Y., Hua, S., Jia, R., Huang, J., 2019b. Effect of aerosols on the ice cloud properties over the Tibetan Plateau. J. Geophys. Res. Atmos. 124 https://doi.org/10.1029/2019JD030463.

Liu, Y., Zhu, Q., Wang, R., Xiao, K., Cha, P., 2019c. Distribution, source and transport of the aerosols over Central Asia. Atmos. Environ. 210, 120–131. https://doi.org/10.1016/j.atmosenv.2019.04.052.

Liu, Y., Luo, R., Zhu, Q., Hua, S., Wang, B., 2019d. Cloud ability to produce precipitation over arid and semiarid regions of central and East Asia. Int. J. Climatol. 1–14. https://doi.org/10.1002/joc.6304.

Liu, Y., Li, Y., Huang, J., Zhu, Q., Wang, S., 2020. Attribution of the Tibetan plateau to northern drought. Natl. Sci. Rev. https://doi.org/10.1093/nsr/nwz191.

Lu, Z., Liu, X., Zhang, Z., Zhao, C., Penner, J.E., 2018. Biomass smoke from southern Africa can significantly enhance the brightness of stratocumulus over the southeastern Atlantic Ocean. P. Natl. Acad. Sci. USA. 115 (12), 201713703. https://doi.org/10.1073/pnas.1713703115.

Meehl, G.A., Arblaster, J.M., Collins, W.D., 2008. Effects of black carbon aerosols on the Indian monsoon. J. Clim. 21, 2869–2882. https://doi.org/10.1175/2007JCLI1777.1.

Min, Q., Li, R., Lin, B., Joseph, E., Wang, S., Hu, Y., Morris, V., Chang, F., 2009. Evidence of mineral dust altering cloud microphysics and precipitation. Atmos. Chem. Phys. 9, 3223–3231. https://doi.org/10.5194/acp-9-3223-2009.

Miyamoto, Y., Kajikawa, Y., Yoshida, R., Yamaura, T., Yashiro, H., Tomita, H., 2013. Deep moist atmospheric convection in a sub kilometer global simulation. Geophys. Res. Lett. 40, 4922–4926. https://doi.org/10.1002/grl.50944.

Morrison, H., Grabowski, W.W., 2011. Cloud-system resolving model simulations of aerosol indirect effects on tropical deep convection and its thermodynamic environment. Atmos. Chem. Phys. 11, 10503–10523. https://doi.org/10.5194/acp-11-10503-2011.

Myhre, G., Stordal, F., Johnsrud, M., Kaufman, Y.J., Rosenfeld, D., Storelvmo, T., Kristjansson, J.E., Berntsen, T.K, Myhre, A., Isaksen, I.S.A.., 2007. Aerosol-cloud interaction inferred from MODIS satellite data and global aerosol models. Atmos. Chem. Phys. 7 (12), 3081–3101. https://doi.org/10.5194/acp-7-3081-2007.

Niwa, Y., Patra, P.K., Sawa, Y., Machida, T., Matsueda, H., Belikov, D., Maki, T., Ikegami, M., Imasu, R., Maksyutov, S., Oda, T., Satoh, M., Takigawa, M., 2011a. Three-dimensional variations of atmospheric CO_2: aircraft measurements and multi-

transport model simulations. Atmos. Chem. Phys. 11, 13359–13375. https://doi.org/10.5194/acp-11-13359-2011.
Niwa, Y., Tomita, H., Satoh, M., Imasu, R., 2011b. A three-dimensional icosahedral grid advection scheme preserving monotonicity and consistency with continuity for atmospheric tracer transport. J. Meteorol. Soc. Jpn. 89, 255–268. https://doi.org/10.2151/jmsj.2011-306.
Petters, M.D., Snider, J.R., Stevens, B., Vali, G., Faloona, I., Russell, L.M., 2006. Accumulation mode aerosol, pockets of open cells, and particle nucleation in the remote subtropical Pacific marine boundary layer. J. Geophys. Res. Atmos. 111, D02206. https://doi.org/10.1029/2004JD005694.
Platnick, S.M., King, M.D., Ackerman, S.A., Menzel, W.P., Frey, R.A., 2003. The MODIS cloud products: algorithms and examples from terra. IEEE. T. Geosci. Remote. 41 (2), 459–473. https://doi.org/10.1109/TGRS.2002.808301.
Pokharel, M., Guang, J., Liu, B., Kang, S.C., Ma, Y.M., Holben, B.N., Xia, X.A., Xin, J.Y., Ram, K., Rupakheti, D., Wan, X., Wu, G.M., Bhattarai, H., Zhao, C., Cong, Z.Y., 2020. J. Geophys. Res. Atmos. 124 (23), 13357–13374. https://doi.org/10.1029/2019jd031293.
Rajeev, K., Ramanathan, V., Meywerk, J., 2000. Regional aerosol distribution and its long-range transport over the Indian Ocean. J. Geophys. Res. Atmos. 105 (D2), 2029–2044. https://doi.org/10.1029/1999JD900414.
Ramanathan, V., Chung, C., Kim, D., Bettge, T., Buja, L., Kiehl, J.T., Washington, W.M., Fu, Q., Sikka, D.R., Wild, M., 2005. Atmospheric brown clouds: impacts on south Asian climate and hydrological cycle. P. Natl. A. Sci. 102 (15), 5326–5333. https://doi.org/10.1073/pnas.0500656102.
Remer, L.A., Kaufman, Y.J., Tanré, D., Mattoo, S., Chu, D.A., Martins, J.V., Li, R.R., Ichoku, C., Levy, R.C., Kleidman, R.G., Eck, T.F., Vermote, E., Holben, B.N., 2005. The MODIS aerosol algorithm, products, and validation. J. Atmos. Sci. 62 (4), 947–973. https://doi.org/10.1175/JAS3385.1.
Roh, W., Satoh, M., 2014. Evaluation of precipitating hydrometeor parameterizations in a single-moment bulk microphysics scheme for deep convective systems over the Tropical Central Pacific. J. Atmos. Sci. 71, 2654–2673. https://doi.org/10.1175/JAS-D-13-0252.1.
Rosenfeld, D., Rudich, Y., Lahav, R., 2001. Desert dust suppressing precipitation: a possible desertification feedback loop. Proc. Natl. Acad. Sci. U.S.A. 98, 5975–5980. https://doi.org/10.1073/pnas.101122798.
Rosenfeld, D., Lohmann, U., Raga, G.B., O'Dowd, C.D., Kulmala, M., Fuzzi, S., Reissell, A., Andreae, M.O., 2008. Flood or drought: how do aerosols affect precipitation? Science 321, 1309. https://doi.org/10.1126/science.1160606.
Rosenfeld, D., Yu, X., Liu, G., Xu, X., Zhu, Y., Yue, Z., Dai, J., Dong, Z., Dong, Y., Peng, Y., 2011. Glaciation temperatures of convective cloud singe sting desert dust, air pollution and smoke from forest fires. Geophys. Res. Lett. 38, L21804. https://doi.org/10.1029/2011GL049423.
Saito, T., Hayasaka, T., 2014. Effects of dust aerosols on warm cloud properties over East Asia and the sahara from satellite data. J. Meteorol. Soc. Jpn. 92A, 109–123. https://doi.org/10.2151/jmsj.2014-A07.
Sakaeda, N., Wood, R., Rasch, P.J., 2011. Direct and semi-direct aerosol effects of southern African biomass burning aerosol. J. Geophys. Res. 116, D12205. https://doi.org/10.1029/2010JD015540.
Satoh, M., Matsuno, T., Tomita, H., Miura, H., Nasuno, T., Iga, S., 2008. Nonhydrostatic icosahedral atmospheric model (NICAM) for global cloud resolving simulations. J. Comput. Phys. 227, 3486–3514. https://doi.org/10.1016/j.jcp.2007.02.006.
Satoh, M., Tomita, H., Yashiro, H., Miura, H., Kodama, C., Seiki, T., Noda, A.T., Yamada, Y., Goto, D., Sawada, M., Miyoshi, T., Niwa, Y., Hara, M., Ohno, T., Iga, S.-i., Arakawa, T., Inoue, T., Kubokawa, H., 2014. The non-hydrostatic icosahedral atmosphericmodel: description and development. Prog. Earth Planet. Sc. 1 (18) https://doi.org/10.1186/s40645-104-0018-1.
Segal, M., Weaver, J., Purdom, J.F.W., 1989. Some effects of the Yellowstone fire smoke plume on northeast Colorado at the end of summer 1988. Mon. Weather Rev. 117, 2278–2283. https://doi.org/10.1175/1520-0493.
Sokolik, I.N., Toon, O.B., 1996. Direct radiative forcing by anthropogenic airborne mineral aerosols. Nature 381, 681–683. https://doi.org/10.1038/381681a0.
Suzuki, K., Nakajima, T., Satoh, M., Tomita, H., Takemura, T., Nakajima, T.Y., Stephens, G.L., 2008. Global cloud-system-resolving simulation of aerosol effect on warm clouds. Geophys. Res. Lett. 35610–35616. https://doi.org/10.1029/2008GL035449.
Suzuki, K., Stephens, G.L., van den Heever, S.C., Nakajima, T.Y., 2011. Diagnosis of the warm rain process in cloud-resolving models using Joint CloudSat and MODIS observations. J. Atmos. Sci. 68, 2655–2670. https://doi.org/10.1175/JAS-D-10-05026.1.
Takemura, T., Okamoto, H., Maruyama, Y., Numaguti, A., Higurashi, A., Nakajima, T., 2000. Global three-dimensional simulation of aerosol optical thickness distribution of various origins. J. Geophys. Res. 105, 17853–17873. https://doi.org/10.1029/2000jd900265.
Takemura, T., Egashira, M., Matsuzawa, K., Ichijo, H., O'Ishi, R., Abe-Ouchi, A., 2009. A simulation of the global distribution and radiative forcing of soil dust aerosols at the Last Glacial Maximum. Atmos. Chem. Phys. 9, 3061–3073. https://doi.org/10.5194/acp-9-3061-2009.
Tao, W.K., Chen, J.P., Li, Z., Wang, C., Zhang, C., 2012. Impact of aerosols on convective clouds and precipitation. Rev. Geophys. 50, RG2001. https://doi.org/10.1029/2011RG000369, 2012.
Tomita, H., 2008a. New microphysical schemes with five and six categories by diagnostic generation of cloud ice. J. Meteorol. Soc. Jpn. 86A, 121–142. https://doi.org/10.2151/jmsj.86A.121.
Tomita, H., 2008b. A stretched icosahedral grid by a new grid transformation. J. Meteorol. Soc. Jpn. 86A, 107–119. https://doi.org/10.2151/jmsj.86A.107.
Tomita, H., Satoh, M., 2004. A new dynamical framework of nohydrostatic global model using the icosahedral grid. Fluid Dynam. Res. 34, 357–400. https://doi.org/10.1016/j.fluiddyn.2004.03.003.
Twomey, S., 1977. The influence of pollution on the shortwave albedo of clouds. J. Atmos. Sci. 34 (7), 1149–1152. https://doi.org/10.1175/1520-0469(1977)034<1149:TIOPOT>2.0.CO;2.
Uchida, J., Mori, M., Nakamura, H., Satoh, M., Suzuki, K., Nakajima, T., 2016. Error and energy budget analysis of a nonhydrostatic stretched-grid global atmospheric model. Mon. Weather Rev. 144 (4), 1423–1447. https://doi.org/10.1175/MWR-D-15-0271.1.
van den Heever, S.C., Carrio, G.G., Cotton, W.R., DeMott, P.J., Prenni, A.J., 2006. Impacts of nucleating aerosol on Florida storms. Part I: mesoscale simulations. J. Atmos. Sci. 63, 1752–1775. https://doi.org/10.1175/JAS3713.1.
Wang, W., Huang, J., Minnis, P., Hu, Y., Li, J., Huang, Z., Ayers, J.K., Wang, T., 2010. Dusty cloud properties and radiative forcing over dust source and downwind regions derived from A-train data during the pacific dust experiment. J. Geophys. Res. Atmos. 115 (D4) https://doi.org/10.1029/2010JD014109.
Wang, Q., Li, Z., Guo, J., Zhao, C., Cribb, M., 2018. The climate impact of aerosols on the lightning flash rate: is it detectable from long-term measurements? Atmos. Chem. Phys. 18 (17), 12797–12816. https://doi.org/10.5194/acp-18-12797-2018.
Xie, S., Liu, X., Zhao, C., Zhang, Y., 2013. Sensitivity of CAM5-simulated arctic clouds and 18 radiation to ice nucleation parameterization. J. Clim. 26, 5981–5999. https://doi.org/10.1175/JCLI-D-12-00517.1.
Yang, X., Zhao, C., Zhou, L.J., Wang, Y., Liu, X.H., 2016a. Distinct impact of different types of aerosols on surface solar radiation in China. J. Geophys. Res. Atmos. 121 (11), 6459–6471. https://doi.org/10.1002/2016JD024938.
Yang, X., Zhao, C., Guo, J., Wang, Y., 2016b. Intensification of aerosol pollution associated with its feedback with surface solar radiation and winds in Beijing. J. Geophys. Res. Atmos. 121 (8), 4093–4099. https://doi.org/10.1002/2015JD024645.
Yang, J., Duan, K., Kang, S., Shi, P., Ji, Z., 2017. Potential feedback between aerosols and meteorological conditions in a heavy pollution event over the Tibetan Plateau and Indo-Gangetic Plain. Clim. Dynam. 48 (9–10), 2901–2917. https://doi.org/10.1007/s00382-016-3240-2.
Yang, X., Zhao, C., Zhou, L., Li, Z., Cribb, M., Yang, S., 2018a. Wintertime cooling and a potential connection with transported aerosols in Hong Kong during recent decades. Atmos. Res. 211 (OCT.), 52–61. https://doi.org/10.1016/j.atmosres.2018.04.029.
Yang, X., Zhou, L., Zhao, C., Yang, J., 2018b. Impact of aerosols on tropical cyclone-induced precipitation over the mainland of China. Climatic Change 148, 173–185. https://doi.org/10.1007/s10584-018-2175-5.
Ying, M., Zhang, W., Yu, H., Lu, X., Feng, J., Fan, Y., Zhu, Y., Chen, D., 2014. An overview of the China meteorological administration tropical cyclone database. J. Atmos. Ocean. Technol. 31 (2), 287–301. https://doi.org/10.1175/JTECH-D-12-00119.1.
Yuan, T., Chen, S., Huang, J., Wu, D., Lu, H., Zhang, G., Ma, X.J., Chen, Z., Luo, Y., Ma, X. H., 2019. Influence of dynamic and thermal forcing on the meridional transport of taklimakan desert dust in spring and summer. J. Clim. 32, 749–767. https://doi.org/10.1175/JCLI-D-18-0361.1.
Zhang, X.Y., Arimoto, R., Cao, J.J., An, Z.S., Wang, D., 2001. Atmospheric dust aerosol over the Tibetan Plateau. J. Geophys. Res. Atmos. 106, 18471–18476. https://doi.org/10.1029/2000JD900672.
Zhang, R., 2010. Getting to the critical nucleus of aerosol formation. Science 328, 1366–1367. https://doi.org/10.1126/science.1189732.
Zhang, K., Gao, H., 2007. The characteristics of Asian-dust storms during 2000–2002: from the source to the sea. Atmos. Environ. 41, 9136–9145. https://doi.org/10.1016/j.atmosenv.2007.08.007.
Zhao, C., Garrett, T.J., 2015. Effects of arctic haze on surface cloud radiative forcing. Geophys. Res. Lett. 42 (2), 557–564. https://doi.org/10.1002/2014GL062015.
Zhao, C., Lin, Y.L., Wu, F., Wang, Y., Li, Z.Q., Rosenfeld, D., Wang, Y., 2018. Enlarging rainfall area of tropical cyclones by atmospheric aerosols. Geophys. Res. Lett. 45 (16), 8604–8611. https://doi.org/10.1029/2018GL079427.
Zhao, C., Yang, Y., Fan, H., Huang, J., Fu, Y., Zhang, X., Kang, S., Cong, Z., Letu, H., Menenti, M., 2020. Aerosol characteristics and impacts on weather and climate over the Tibetan Plateau. Nati. Sci. Rev. https://doi.org/10.1093/nsr/nwz184.
Zhou, X., Bei, N., Liu, H., Cao, J., Xing, L., Lei, W., Molina, L., Li, G., 2017. Aerosol effects on the development of cumulus clouds, over the Tibetan Plateau. Atmos. Chem. Phys. 17 (12), 7423–7434. https://doi.org/10.5194/acp-17-7423-2017.
Zhu, Q., Liu, Y., Jia, R., Hua, S., Shao, T., Wang, B., 2018. A numerical simulation study on the impact of smoke aerosols from Russian forest fires on the air pollution over Asia. Atmos. Environ. 182, 263–274. https://doi.org/10.1016/j.atmosenv.2018.03.052.
Zhu, Q., Liu, Y., Shao, T., Tang, Y., 2020. Transport of asian aerosols to the pacific ocean. Atmos. Res. 234, 104735. https://doi.org/10.1016/j.atmosres.2019.104735.